Mexican Journal of Phytopathology
e-ISSN: 2007-8080

Crossref Open access

Scientific Article

Distribution of *Candidatus* Liberibacter asiaticus in the canopy and roots of *Citrus sinensis* under asymptomatic condition

Gustavo Mora-Aguilera*[1], Gerardo Acevedo-Sánchez[1], Verónica Martínez-Bustamante[1], Viridiana López-Bautista[1], Ma. Alejandra Gutiérrez-Espinosa[2], Pedro Robles-García[3]. [1]Laboratorio de Análisis de Riesgo Epidemiológico Fitosanitario (CP-LANREF), [2]Fruticultura, Colegio de Postgraduados, Carretera México-Texcoco Km. 36.5, Montecillo, Texcoco CP. 56264, Estado de México. [3]SENASICA-DGSV. Av. Insurgentes Sur 489, Hipódromo, Cuauhtémoc, CP. 06100, CDMX.

***Corresponding Author:**
Gustavo Mora-Aguilera
morag@colpos.mx

Section:
Periodical Issue

***Received*:**
June 20, 2025
***Accepted*:**
December 20, 2025
***Published*:**
December 27, 2025
Early Access 2026

Citation:
Mora-Aguilera G, Acevedo-Sánchez G, Martínez-Bustamante V, López-Bautista V, Gutiérrez-Espinosa MA, and Robles-García P. 2026 Distribution of *Candidatus* Liberibacter asiaticus in the canopy and roots of *Citrus sinensis* under asymptomatic condition. Mexican Journal of Phytopathology 44(1): 109. https://doi.org/10.18781/R.MEX.FIT.2506-2

ABSTRACT

Background/Objective. This study analyzed for the first time the asymptomatic condition induced by *C*Las in *Citrus sinensis* / *C. aurantium* based on initial reports in the Central Gulf region of Mexico. The objective was to analyze with a mechanistic approach the spatial-temporal concentration of *C*Las at the plant level in commercial orchards to demonstrate the possible implication of a prolonged *incubation period* (*IP*) in the asymptomatic expression of HLB.

Materials and Methods. Two out of three trees (A1-A3) (>30 years old) of asymptomatic Valencia sweet orange trees positive for *C*Las, identified through official diagnostic protocols in San José Acateno, Puebla, were confined. On trees A2 and A3, 13 and 16 secondary branches were marked, with a total of 112 and 108 foliage/samples per month, respectively (total 1540 samples), obtained from the distal and proximal parts of each branch. Seven monthly samplings of plant material were carried out between May and December. At the root level, three categories were sampled by diameter/function and by a combination of six distal trunk sectors (0 - 280 cm) by 4 in depth (0 x 110 cm) with a total of 111 samples. DNA extraction was performed with 2% CTAB and quantification by qPCR (oligos, HLBp/HLBas).

Results. In canopy, the incidence / branche in A3 was 52.2% (Ct = 22.7 – 34.9), and in A2 47.8% (Ct = 23.4 – 35), with no statistical difference (p = 0.48). The inoculum load was 1.6 (±1.3) log-*C*Las, equivalent to 109 copies/reaction in 100 mL (range in number of copies 6.3 to 68,870.7). *C*Las did not differ between distal (1.6 *log*) and proximal (1.5 log) samples (p = 0.33). Significative temporal fluctuation was found between June and October in positive samples (37 – 87, $p < 0.0001$), but not in *C*Las concentration (1.6 – 3.5 log-*C*Las, $p > 0.72$). The distribution of *C*Las by branch had a temporal effect (p = 0.0001) and by sector (p = 0.07), showing high mobility and seasonality. The maximum concentration ($\mathbf{Y}_{max}$) was associated with the middle-upper sector of the canopy, and high mobility towards the lower and upper sectors in $\mathbf{Y}_{initial}$ and $\mathbf{Y}_{final}$. In roots, 38.7% positivity was found. The detectability of *C*Las was homogeneous among root types ($p < 0.0001$) but variable in concentration (p = 0.04). The 47.6, 15.4, and 38.7% incidence was associated with 38.3, 43.4, and 9.5 average *C*Las copies for *support*, *conduction*, and *absorption* roots, respectively (p = 0.0001). Two sections with higher *C*Las intensity-concentration (80 – 144 copies) were associated with roots in the middle drip zone (160 – 240 cm) and medium depth strata (50 – 80 cm).

Conclusion. *C*Las was significantly and consistently detected in plant and root tissue throughout the experimental period, but at fluctuating, non-incremental concentration, analogous between trees A2 and A3. The wide canopy-root distribution suggests a chronic systemic effect. Consequently, the *incubation period* does not determine the asymptomatic condition in the sweet orange/sour orange productive system investigated. Other factors, *e.g.* inherent to pathogen variability, could be involved. These results contribute to optimizing a surveillance-monitoring system considering seasonality, zone-branch, sector-canopy and type of tissue, with a greater probability of detection of *C*Las even in an eventual asymptomatic condition and generate new insights for *C*las management. This is the first work that analyzes *PI* mechanistically, at canopy and root level, in initial detections in Mexico of asymptomatic-HLB in productive adult trees of Valencia *C. sinensis* / *C. aurantium* under field conditions.

Keywords: *C*Las, HLB, Inoculum load, Sweet orange, Sour orange

INTRODUCTION

Huanglongbing or HLB caused by *Candidatus* Liberibacter asiaticus (*C*Las) was detected in Yucatán, Mexico, in July 2009. It is currently present in 352 municipalities in 23 commercial citrus-producing states (https://goo.su/qwSbCa - 2025, www.gob.mx -; SENASICA, 2022). During the initial phase of the epidemic (2009-2014), two scenarios predominated: 1) in the Pacific region, with high intensity, prevalence, and inoculum load in vector-plant associated with commercial orchards, predominantly *Citrus aurantifolia*, and 2) in the Yucatan Peninsula with moderate-low intensity, prevalence, and vector-plant inoculum load in *Citrus latifolia* backyards (Mora-Aguilera *et al*., 2014; Flores-Sánchez *et al*., 2015). However, during the regional and intraregional dispersal phase of the vector and the disease (2015-2018), differential epidemic scenarios in terms of incidence and endemicity occurred under specific regional conditions of production, management, climate, among others, *e.g.*, Central Gulf with sweet citrus in commercial and backyard areas (*C. sinensis*, *C. reticulata*, among others) or Northeast with high-yield commercial orchards of *C. sinensis* and *C. reticulata*.

In Mexico, published epidemiological results and indicators on intra-plot or regional dispersion of the *C*Las-*Diaphorina citri* (*Dc*) complex (Gottwald *et al*., 2014; Bassanezi *et al*., 2005; 2013a; Esquivel-Chávez, 2011; Márquez *et al*., 2011), temporal epidemic rates (Mora-Aguilera *et al*., 2014; Bassanezi *et al*., 2005; 2013a; Robles-González *et al*., 2013; Esquivel-Chávez, 2011), regional dispersion scenarios (Flores-Sánchez *et al*., 2017; Mora-Aguilera *et al*., 2014; Robles-González *et al*., 2013), among others, were used to establish official strategies for sampling, monitoring, delimitation, and control of outbreaks through Regional *Dc* Control Areas (ARCOs) under symptomatic conditions (Flores-Sánchez *et al*., 2017; Mora-Aguilera *et al*., 2014; Bassanezi *et al*., 2013a; DGSV-SENASICA, 2010).

A novel scenario arose in Mexico following the detection of five *C*Las - positive plant samples of *C. sinensis* from asymptomatic trees in commercial orchards in S.J. Acateno, Puebla (SENASICA, 2012; 2015). No characteristic HLB symptoms at the Mexican conditions were observed, such as vein clearing, diffuse mottling, or generalized light yellowing (Esquivel-Chávez *et al*., 2012). Interestingly, this condition prevailed until December 2015 (2.5 years), longer than reported for an asymptomatic condition associated with the *incubation period* of *C*Las (Canale *et al*., 2020; Lopes *et al*., 2009).

In this context, the General Direction of Plant Health (DGSV), associated to the National Service for Plant health, Food security, and Agri-food Quality (SENASICA) in Mexico requested to the Laboratory for Phytosanitary Epidemiological Risk Analysis (CP-LANREF) to confine two *Citrus sinensis* trees positive for *C*Las and to develop a research approach to explain this asymptomatic condition.

This study analyzes one of five hypotheses investigated simultaneously to explain the asymptomatic condition induced by *C*Las in *Citrus sinensis* / *C. aurantium* in the Central Gulf of Mexico. The objective was to analyze the spatio-temporal concentration of *C*Las at the plant canopy – root level under commercial conditions to demonstrate the possible implication of a prolonged *incubation period* in the asymptomatic HLB condition, under the premise that the bacterial concentration should be incremental and gradually must exhibit chronic systemic infection throughout an infection-*incubation period*.

MATERIALS AND METHODS

Confinement of asymptomatic plants. In December 2013, two commercial Valencia sweet orange trees (*Citrus sinensis*) positive for *Candidatus* Liberibacter asiaticus (*C*Las), confirmed by RT-PCR protocol, were caged for confinement to study the asymptomatic condition in sweet orange / sour orange, and avoid vectoring reinfection and spreading of the detected *C*Las isolate. Metal structures measuring 8 x 8 x 8 m (length x width x height) protected with double aphid netting were used, following specifications defined by the DGSV-CNRF (Figure 1A). Each structure was fitted with a padlocked door to restrict access to researchers and official personnel. Two HOBO u23 Pro v2 data loggers were installed to record temperature (°C) and relative humidity (RH) variables inside and outside the confinement structure for each tree (Figure 1B). Additionally, a Davis® (Vantage Pro 2 Plus) weather station was installed to measure precipitation, evapotranspiration, solar radiation, and other complementary variables (Figure 1C). During the experiment, weeds were removed mechanically and no agrochemicals were applied. Irrigation was seasonal.

Figure 1. HLB-asymptomatic qPCR *C*Las positive Valencia *Citrus sinensis* / *C. aurantium* orange tree confinement. **A.** Metal confinement structure (8 x 8 x 8 m) with aphid-proof netting. The structures included a key-restricted access door; **B.** HOBO U23 Pro V2 sensor for temperature (°C) and relative humidity (RH), programmed to take measurements at 30-minute intervals withing the confinement area; **C.** Davis Vantage weather station for measuring complementary climate variables such as precipitation, wind speed and direction, evapotranspiration, etc.

Selection and sampling of plant tissue. A total of 13 and 16 primary branches were marked on trees A2 and A3, respectively (Figure 2A). The branches were numbered clockwise in a west-east direction (Figure 2B). For each primary branch, secondary branches were selected and marked specifically for leaf sampling. Due to the timing of the experiment outside the main vegetative growth periods, secondary branches were selected directly based on the availability of plant tissue optimal for molecular analysis. Leaf samples were collected from the distal and proximal regions (Figure 2C). For distal samples, recent vegetative growth was identified and expanded leaflet was taken, and for proximal samples, a leaf was collected from the vegetative shoot of the previous growing cycle. All samples were labeled and kept cold in the field and laboratory. For qPCR analysis, the central leaf vein was used. Sampling was conducted monthly between May and December 2014. A total of 1 540 samples were analyzed.

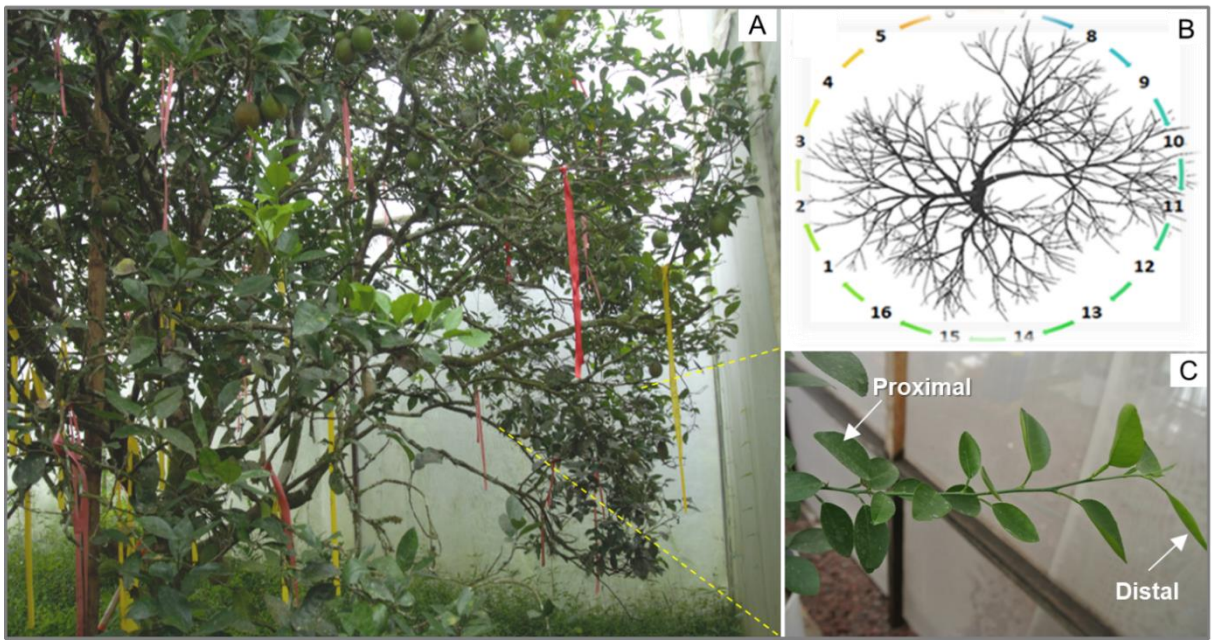

Figure 2. A. Valencia *C. sinensis* / *C. aurantium* tree HLB-asymptomatic *C*Las-positive confined in cages with aphid-proof netting. The red and yellow strips show the selection and marking of primary (red) and secondary (yellow) branches for proximal or distal section monthly sampling from May - December. **B.** Example of the method for numbering branches in clockwise order. **C.** Structure of a citrus branch for selection of proximal and distal leaves. A total of 1540 samples were qPCR analyzed / A2 and A3 trees.

Root sampling. For root sampling, from the truck base, a 55° triangle was marked on the soil surface, dividing five sections every 40 cm (Figure 3A-B). Subsequently, 20 cm deep sections were dug for the first stratum A (0 to 20 cm), while for the next three strata, 30 cm deep sections were dug (B = 20 - 50 cm, C = 50 - 80 cm, D = 80 - 110 cm) (Figure 3C-D). Root samples were collected for each section-stratum and classified according to their structure and function: *support* (S), *conduction* (C), and *absorption* (AB). In each stratum, the soil was sifted to separate the total root mass. The samples were stored in polypropylene bags and kept in a cooler. In the laboratory, each sample was washed with water to remove soil residues.

The root samples were separated into the previously defined classification (S, C, and AB) and disinfected with 1% sodium hypochlorite (NaClO) for 1 min. They were then rinsed twice with distilled water. From the *conducting* and *supporting* roots, the cortex (phloem) was removed and ground with liquid nitrogen in a mortar. The absorbing roots were ground using all the available tissue. For each section-stratum at least three subsamples were analyzed for a total of 111.

Molecular analysis, diagnosis, and quantification of *C*Las. Total DNA extraction from plant and root samples was performed using the 2% CTAB method with saline buffer from 100 mg of plant and root material. Quantification by qPCR was performed on StepOne™ (Applied Biosystems®, Foster City, CA) using the standard curve method, using the HLBp oligos (5'- GCG TTA TCC CGT AGA AAA AGG TAG -3'), HLBas (5'- TCG AGC GCG TAT GCA ATA CG -3') and the Taqman probe (5'- AGA CGG GTG AGT AAC GCG -3') (Li *et al*., 2006). The reaction consisted of a thermal cycling program of 95 °C for 3 min, 40 cycles of 95 °C for 5 s; 59 °C for 40 s and 59 °C for 35 s. Samples that reported 8 to 35 thermocycling cycles (*Ct* for *Cycle threshold*) exceeding the optimal fluorescence threshold were considered *positive*. Samples with *Ct* >35 were considered *negative*.

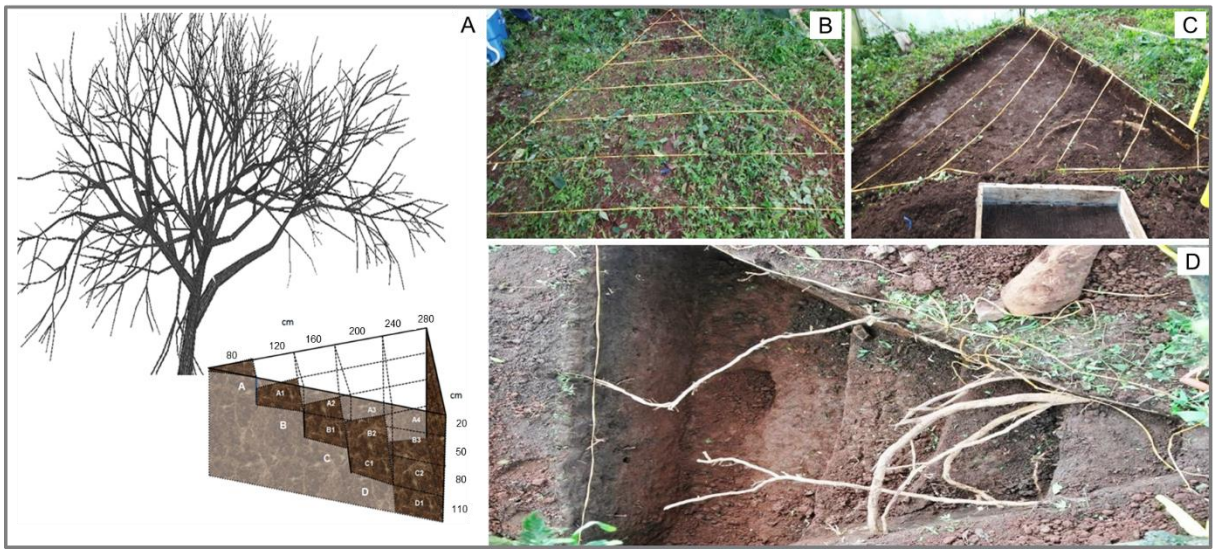

Figure 3. 3D-sectional system used for root sampling of HLB-asymptomatic qPCR positive A3-tree of *C. sinensis* / *C. auranium*. **A.** Design used for root sampling considering the distance proximal to the trunk and up to the drip zone (0 - 280 cm) and four depths (0 - 110 cm). **B.** Design and marking of the excavation strata. **C.** Delimitation of the excavation area and soil sifting from different strata. **D.** Excavated sections for three type-root sampling used in *C*Las quantification by qPCR. A total of 24 bulk soil sections were sampled (6 x 4) and 111 samples qPCR analyzed.

An external calibration curve was generated to quantify the number of genomic *C*Las copies in samples. The fragment of the 16S rDNA gene cloned into a plasmid (PGEM-T ® Promega®) was used, which was purified and quantified by UV spectrophotometry (Nanodrop 1000) with serial dilutions. These were amplified with three replicates per concentration, and a logarithmic regression was used to estimate the *C*Las concentration, (y) = 41.95 - 3.37 (Log Staring Quantity) (r^2=1, efficiency 97.9%), y = Ct, which calculates the number of copies of the 16S rDNA gene. To reduce the effect of variability and for the purpose of comparing DNA concentrations, a dilution to 20 ng μL^{-1} was performed.

Parameterization and epidemiological analysis. qPCR results were integrated into a temporal epidemiological matrix. *C*Las epidemic curves were constructed using *C*Las copy quantification (Q) and the number of positive samples over time at monthly intervals. Three occurrence windows were parameterized per *C*Las epidemic curve: $\mathbf{Y}_i$ as the initial sampling (t = 0), characterized by a period of pre-rainwater stress; $\mathbf{Y}_{max}$ as the period of highest inoculum load in the plant; and $\mathbf{Y}_f$ as the final phase of the *C*Las epidemic curve. The parameterization was performed by tree, branch, and distal or proximal sampling section. Geospatial vector maps of Q and $log(Q)$ interpolated by epidemic occurrence window ($\mathbf{Y}_i$, $\mathbf{Y}_{max}$, and $\mathbf{Y}_f$) and by root structure (*support, conduction*, and *absorption*) were processed and analyzed in Golden Surfer®v10. ANOVA and Tukey mean comparison (p = 0.05) analyses were conducted in SAS 9.4.

RESULTS

Detection and quantification of *C*Las in canopy. Seven monthly samplings were made between May and December 2014. A total of 1 540 samples were analyzed by qPCR, 784 from tree 2 (A2) and 756 from tree 3 (A3) (Table 1). A 41.9 % (646 samples) of the total samples analyzed were positive for *C*Las with a *Ct* threshold of 22.7 – 35. There were no statistical differences in positivity between trees (p = 0.48), with A3 obtaining 52.2% (337 positive, *Ct* = 22.7 – 34.9) and A2 47.8% (309 positive, *Ct* = 23.4 – 35). At the intra-branch

sampling level, positivity in distal samples was slightly higher at 50.9% (329) compared to proximal samples, which had an incidence of 49.1% (317). The positivity of *C*Las in the distal branch area was not different in confined trees (A2 = 164; A3 = 165) (p = 0.97). In the proximal branch sector, A3 had a higher number of positive samples (173) than the distal (164) (p = 0.48). In A2, the incidence was lower but similar in trend (distal = 165; proximal = 144) (p = 0.42). The relative incidence of *C*Las per tree was higher in A3 with 49.5% compared to 39.4% in A2 (p = 0.68). By sampling sector, A2 had a positivity rate of 53.4 and 46.6% in the distal and proximal zones, respectively. The incidence in A3 was higher in the proximal zone with 51.3 vs. 48.7% in the distal zone (Table 1).

Table 1. Comparison of the number of qPCR positive samples in seven monthly dates carried out on HLB-asymptomatic canopy of *Citrus sinensis* Valencia trees (A2 and A3) during May–December, and inoculum load distribution (*C*Las) in proximal and distal sections on selected and marked branches for bacterium monitoring.

Sampling date	Positive samples[x] (Log[Q *C*Las])[y]		Number of positive samples per branch sector (Log[Q *C*Las])			
			Distal		*Proximal*	
	A2	*A3*	*A2*	*A3*	*A2*	*A3*
May 27	3 (0.5 ± 0.8)	12 (1.0 ± 1.2)	9 (1.2 ± 1.3)	0 (0.4 ± 0.8)	3 (0.5 ± 0.8)	3 (0.8 ± 0.9)
June 27	71 (2.0 ± 1.3)	87 (2.6 ± 0.8)	45 (2.7 ± 0.8)	38 (2.3 ± 1.1)	33 (1.8 ± 1.4)	42 (2.6 ± 0.8)
July 25	65 (2.0 ± 1.4)	73 (2.8 ± 1.8)	33 (0.5 ± 0.8)	36 (2.2 ± 1.4)	29 (1.7 ± 1.4)	40 (2.8 ± 1.8)
Aug. 31	36 (0.5 ± 0.8)	78 (2.4 ± 1.2)	35 (2.2 ± 1.1)	19 (1.4 ± 0.8)	17 (1.2 ± 0.9)	43 (2.6 ± 1.3)
Oct. 02	75 (2.0 ± 1.3)	45 (1.5 ± 1.1)	17 (1.4 ± 1.2)	39 (2.3 ± 1.3)	36 (1.7 ± 1.3)	28 (1.7 ± 0.1)
Nov. 06	54 (1.3 ± 0.7)	29 (1.3 ± 0.8)	19 (1.5 ± 0.7)	31 (1.4 ± 0.7)	23 (1.2 ± 0.7)	10 (1.1 ± 0.8)
Dec. 10	5 (0.3 ± 0.6)	13 (0.9 ± 0.7)	6 (0.9 ± 0.8)	2 (0.3 ± 0.6)	3 (0.3 ± 0.6)	7 (0.9 ± 0.7)
Total	**309** (1.3 ± 1.2) (39.4%)	**337** (1.8 ± 1.4) (44.5%)	**165** (1.5 ± 1.3) (53.4%)	**164** (1.8 ± 1.3) (48.7%)	**144** (1.2 ± 1.2) (46.6%)	**173** (1.8 ± 1.4) (51.3%)
A2 + A3	**646** (1.6 ± 1.3) (**41.9%**)		**329** (1.6 ± 1.3) (**50.9%**)		**317** (1.5 ± 1.3) (**49.1%**)	

[x]Total samples by date: 112 tree A2 and 108 tree A3. Total = 1540 samples per experimental period.
[y]Average number of log-*C*Las copies ± standard deviation.

The estimated inoculum load based on the average number of *C*Las copies for 646 positive samples was 1.6 (±1.3) *log*, equivalent to 109 copies/reaction of 100 mL (6.3 to 68 870.7 range). The results showed that *C*Las was not statistically different (p = 0.33) between positive samples from the distal zone (1.6 log-*C*Las) and those from the proximal zone (1.5 log-*C*Las). Per tree, A3 showed a significantly (p < 0.00001) higher inoculum load of 1.8 (±1.3) log-*C*Las, but with no difference between the proximal and distal zones (1.8 log-*C*Las; p = 0.8). A2 had a lower inoculum load of 1.3 (±1.2) log-*C*Las compared to A3 (p < 0.00001). In samples from distal sector, a higher inoculum load of 1.5 (±1.3) log-*C*Las was found than in the proximal zone, with 1.2 (±1.2) log-*C*Las (p = 0.04) (Table 1).

Temporal *C*Las fluctuation in canopy. In general, the period of highest statistically significant incidence was between June and October, with 37 – 87 positive samples (p < 0.0001), accounting for 82% (530) of the total positive samples. In A2, except for August, with 36 samples (17.7%) detected positive, the range of positive samples was 54 – 75 between June and November, accounting for 94% of the total (p = 0.02). Positive samples in May (3) and December (5) were associated with periods of low detectability (p = 0.88). In contrast, A3 had the most inductive period between July and August (p = 0.0003) with a monthly average of 73 – 87 positive samples, accounting for 70.1% of the total. In this tree, October–December was a period of constant decline (p > 0.05) in the detection of positive samples, falling from 45 to 13, respectively. In A3, May and December were again

the significantly least inductive periods with the lowest incidence of positive samples (p = 0.95) (Figure 4A). The fluctuation in *C*Las showed no contrasting differences between trees (p = 0.5) or collection periods (p > 0.72), ranging between 1.6 and 3.5 log-*C*Las for the months of May (A2) and July (A3). A2 had a *C*Las concentration of 1.6 – 2.8 log-*C*Las, with a higher concentration (2.1 – 2.8 log-*C*Las, p = 0.02) associated with the period of highest detectability of positive samples (June–October). In A3, the inoculum load was 1.8 – 3.5 log-*C*Las, higher than in A2 (p = 0.07), with a main peak in July equivalent to 3.5 *log*. The inoculum load showed a decreasing trend like positivity, reducing the *C*Las load from 2.7 to 1.8 between October and December (Figure 4B).

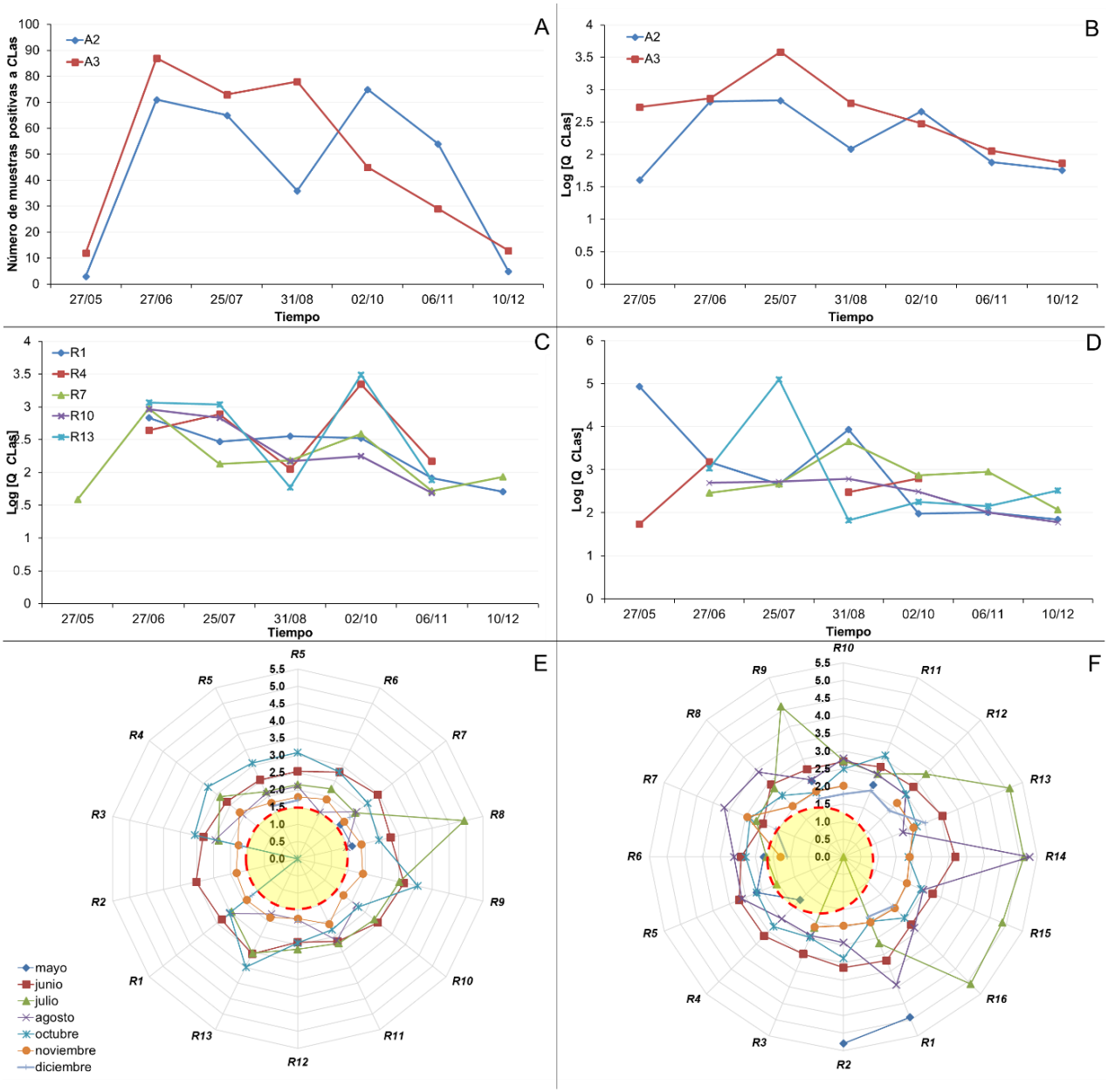

Figure 4. A. Number of qPCR *C*Las positive samples per tree (A2 and A3) detected on seven monthly sampling dates on Valencia *C. sinensis* / *C. aurantium* HLB-asymptomatic. **B.** Temporal fluctuation of bacterial concentration in 21 total branches of trees A2 and A3. **C-D**. Temporal fluctuation of *C*Las at the branch level. The example of 5/13 branches for A2 (**C**) and 5/16 for A3 (**D**) is shown. **E-F**. Temporal fluctuation of *C*Las per branch and A2-tree (**E**) y A3 (**F**). Red dotted circle shows the minimum threshold (log-*C*Las) for quantification of *C*Las copies in positive samples.

The greatest variability of *C*Las fluctuation in canopy was found at the branch (R) and proximal-distal sampling sector (Table 1 and Figure 4). In general, A2 showed homogeneity in the distribution of *C*Las per branch with marginal significant differences (p = 0.07), ranging from 1.5 (May, R7) to 2.8 (October, R13). Branches R4 and R13 occurred at the significantly higher inoculum load peak of 3.4 *log* ($p < 0.02$), diametrically opposite in the canopy. The rest of the branches showed a decreasing trend in *C*Las between August and December ($p = 0.0001$) (Figure 4C).

In A3, although there was high variability in the fluctuation of *C*Las in the canopy of *C. sinensis*, it was not significantly different at the branch level ($p = 0.15$). The branches varied in *C*Las concentration between 1.7 *log* (May, R4) and 5.1 *log* (July, R13). The inoculum load on A3 branches was significantly higher ($p = 0.0001$) between May and August, with 2.4 – 5.1 log-*C*Las, and lower and stable between September and December, with 1.7 – 2.9 log-*C*Las (Figure 4D).

Regarding temporal fluctuation in the period of highest positivity at the branch level, A2 showed greater homogeneity in the distribution of *C*Las (p = 0.07). Except for R8 in July (4.9 log-CLas) and R1 in October (0 log-*C*Las), the rest of the branches behaved homogeneously in the canopy of *C. sinensis*. The intensity of the *C*Las bacterial load varied by collection period, with the highest inoculum load detected in June (2.4 – 3.1 *log*), July (2.1 – 4.9 *log*), and October (2.2–3.6 *log*) ($p = 0.0001$) (Figure 4E).

In A3, the temporal fluctuation of *C*Las per branch was asymmetric, variable, and higher than in A2 ($p = 0.002$). In general, in A3, the bacterial load of *C*Las in July was significantly high, fluctuating, and concentrated in R9 (4.6 *log*) and the R13–R16 sector with 4.9 – 5.1 *log* ($p = 0.0001$). One month later, in August, it was higher in R1 (3.9 log-*C*Las), R7–R8 (3.4 – 3.6log-*C*Las), and R14 (5.3log-*C*Las) ($p = 0.0001$). The rest of the branches had a constant and homogeneous distribution of *C*Las, respectively (Figure 4F).

Canopy *C*Las spatial distribution and directionality at three epidemic stages. Analysis of the temporal fluctuation in positive samples of *C*Las bacterial load at three epidemic stages ($\boldsymbol{Y_i}$, $\boldsymbol{Y_{max}}$, and $\boldsymbol{Y_f}$) identified an asynchronous process of $\boldsymbol{Y_{max}}$ and a heterogeneous distribution at canopy level between A2 and A3 (Figure 5). By epidemic moment, it was shown that in $\boldsymbol{Y_i}$ (May) the distribution of *C*Las copies was concentrated in the middle and lower third of the canopy in A2 (0.08 – 47.2 copies) and A3 (6.8 – 38,842 copies).

The intra-canopy simulation showed southeast-northwest directionality-dispersion of *C*Las with the highest inoculum load (21,187 – 38,842 copies), while bacterial mobility in the rest of the canopy was lower and random (6.8 – 21,187 copies) (Figure 5A). In A2, the highest inoculum load was in the center of the middle third of the canopy with a northeast-southwest directionality (20 – 47.2 copies), and in the rest of the canopy it ranged from 0.08 – 19.9 copies of *C*Las (Figure 5B).

The $\boldsymbol{Y_{max}}$ of *C*Las for A2 and A3 occurred in October and July, respectively, after the onset of rainfall (382.2 mm accumulated). The inoculum load remained higher in A3 (216 – 216,767 copies) than in A2 (9.2 – 4,239 copies) (Figure 5C-D). During this epidemic, the highest concentration and distribution of *C*Las was mainly located in the upper-middle third of the canopy of A3 (65,889 – 216,767 copies) and A2 (1,416 – 4,239 copies). In A3, *C*Las mobility was multidirectional with a predominance of east-west inoculum load (Figure 5C). In A2, the effect on the directionality of the highest *C*Las concentration was mainly south-east (Figure 5D).

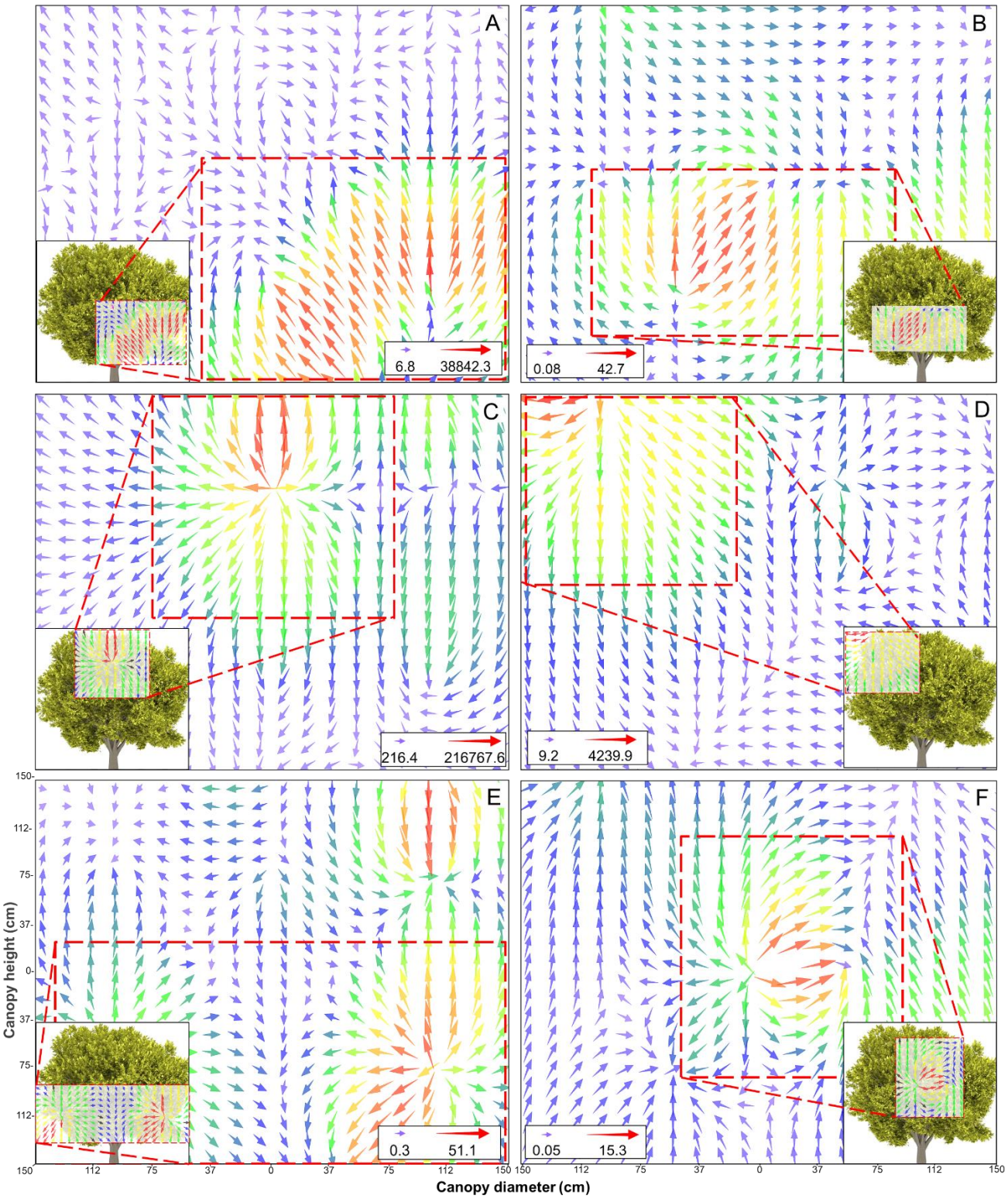

Figure 5. Canopy spatial *C*Las distribution and movement on HLB asymptomatic trees of Valencia *C. sinensis* / *C. aurantium*. **A**, **C**, and **E**. Vector interpolation map representing the bacteria load and directionality for three epidemic moments Y_i (May), Y_{max} (July), and Y_f (December), respectively, in **A3-tree**; and **B**, **D**, and **F** for **A2-tree**. The size and color of vectors show the inoculum load trend in the canopy. On bottom boxes, the numbers of bacterium copies relate to the arrows size and color as reference measure. The directionality of the vector shows a simulation of the movement of the bacteria at the plant canopy level. Remarqued dotted sections indicate a higher *C*Las concentration.

The end of the inoculum load cycle (Y_f) occurred in December in A2 (0.05 – 15.3 copies) and A3 (0.3 – 51.1 copies) (Figure 5F). With a lower bacterial load, Y_f showed agreement in the distribution of *C*Las with respect to the sectors with the highest inoculum in Y_i. In A3, the lower and upper thirds showed multidirectional distribution in the canopy with a south-northeast trend in the lower third (15.5 – 51.1 copies) and an east-west trend in the upper third (19.6 – 49.3 copies) (Figure 5E). In contrast, in A2, the highest concentration of *C*Las (5.9 – 15.3 copies) was associated with the middle third, directly linked to inoculum load in Y_i, while the directionality in the sector with the highest concentration tended to be east-west. In the rest of the canopy, the inoculum load (0.05 – 5.8 copies) showed a random trend with multidirectional distribution in the canopy (Figure 5E).

Spatial *C*Las detection and quantification in the root structure. A total of 111 root samples divided into *support* (30), *conduction* (42), and *absorption* (39) were analyzed by qPCR (Table 2). *C*Las positivity in root samples was 38.7% with thresholds of *Ct* = 32.7 – 35, while on *support, conduction*, and *absorption* was 47.6, 15.4, and 38.7%, respectively.

Table 2. Number and percentage of samples qPCR positive for *C*Las in HLB-asymptomatic *C. sinensis* / *C. aurantium* A3-tree with respect to root type, four soil depths and six distances from the trunk.

Root type	Depth (cm)	Distance from trunk (cm)						Total	%[x]	%[y]	%[z]
		80	120	160	200	220	280				
Absorption (n=39)	20	0/3	0/3	.	0/3	0/3	0/3	0/15	0	0	0
	50	.	0/3	.	0/3	0/3	.	0/9	0	0	0
	80	.	.	0/3	0/3	.	0/3	0/9	0	0	0
	110	.	.	.	3/3	.	3/3	6/6	100	13.9	5.4
Conduction (n=42)	20	1/3	1/3	1/3	0/3	3/3	2/3	8/18	44.4	18.6	7.2
	50	.	2/3	3/3	3/3	0/3	.	8/12	66.7	18.6	7.2
	80	.	.	2/3	1/3	.	0/3	3/9	33.3	6.9	2.7
	110	.	.	.	1/3	.	.	1/3	33.3	2.3	0.1
Support (n=30)	20	2/3	1/3	.	1/3	4/6	.	8/15	53.3	18.6	7.2
	50	.	3/3	.	.	2/3	.	5/6	83.3	11.6	4.5
	80	.	.	.	1/3	.	0/3	1/6	16.6	2.3	0.1
	110	.	.	.	3/3	.	.	3/3	100	6.9	2.7
Total		**3/9**	**7/18**	**6/12**	**13/33**	**9/21**	**5/18**	**43/111**	**-**	**100**	**38.7**
%[v]		**2.7**	**6.3**	**5.4**	**11.7**	**8.1**	**4.5**	**38.7**			
%[w]		**33.3**	**38.9**	**50.0**	**39.4**	**42.9**	**27.8**	**100**			

[v] Incidence of *C*Las positive samples at different distances from the trunk relative to the total samples analyzed (n = 111). [w]Incidence of *C*Las positive samples from different distances from the trunk relative to the subtotal of positive samples (n = 43). [x]Incidence of *C*Las positive samples by depth strata and root type. [y]Incidence of *C*Las positive samples by depth strata and root type relative to the total samples analyzed (n = 111). [z]Incidence of *C*Las positive samples by depth strata and root type relative to the subtotal of positive samples (n = 43). Color represents positivity, being green negative and red de highest detection.

Regarding relative positivity by depth stratum, *support* and *absorption* roots at 110 cm had a 100% incidence (9/9). In *support* and *conduction* roots, 44.4 – 83.7% relative incidence was found at 20 and 40 cm depth, which corresponds to 4.5 – 7.2% of the total samples analyzed (n = 111) and 11.6 – 18.6% of positive samples (n = 43) (Table 2). The highest incidence in samples collected in relation to distance from the trunk was 58.1%, mainly associated with the section between 80 and 120 cm. In general, at 80 – 220 cm, a decreasing positivity gradient was found from 55.6 to 26.7% and an increase to 77.8% at 280 cm from the trunk, specifically associated with a depth of 20 cm. In relative terms, the highest incidence was recorded at 80 and 120 cm from the trunk, with 55.6 and 47.6%, respectively (Table 2). Regarding the *C*Las concentration and distribution by root type, higher concentrations were found in *support* and *conduction* roots, 38.3 (±47.5) and 43.4 (±24.4) copies, respectively, which were statistically different ($p < 0.0001$) from *absorption* roots (9.5 ± 7.2 *C*Las copies) (Figure 6A).

The bacterial load of *C*Las between 80–120 cm from the trunk was stable (22.6 – 33.7 copies), while 160 – 280 cm showed a decreasing gradient from 42.9 to 10.8 copies ($p < 0.0001$) (Figure 6B). In samples analyzed by depth, the gradient was significantly greater ($p = 0.04$) from 20 to 110 cm with 45.2 – 82.8 copies (Figure 6C). In general, *conduction* roots had a higher incidence and *C*Las concentration with 1.3 – 84.3 copies (Table 2), mainly between 20–40 cm from the trunk ($p = 0.01$), and 80 – 160 cm deep ($p > 0.05$) (Figure 6D). In absorption roots, *C*Las was associated with 110 cm from the trunk in combination with 80 – 120 cm depth with 39.8 – 64.1 copies ($p > 0.05$). In *support* roots, they had variable behavior with 3.2 – 144.5 copies, where a sample collected 110 cm from trunk and 80 cm deep had the statistically highest concentration with 144.5 *C*Las copies ($p = 0.001$) (Figure 6D).

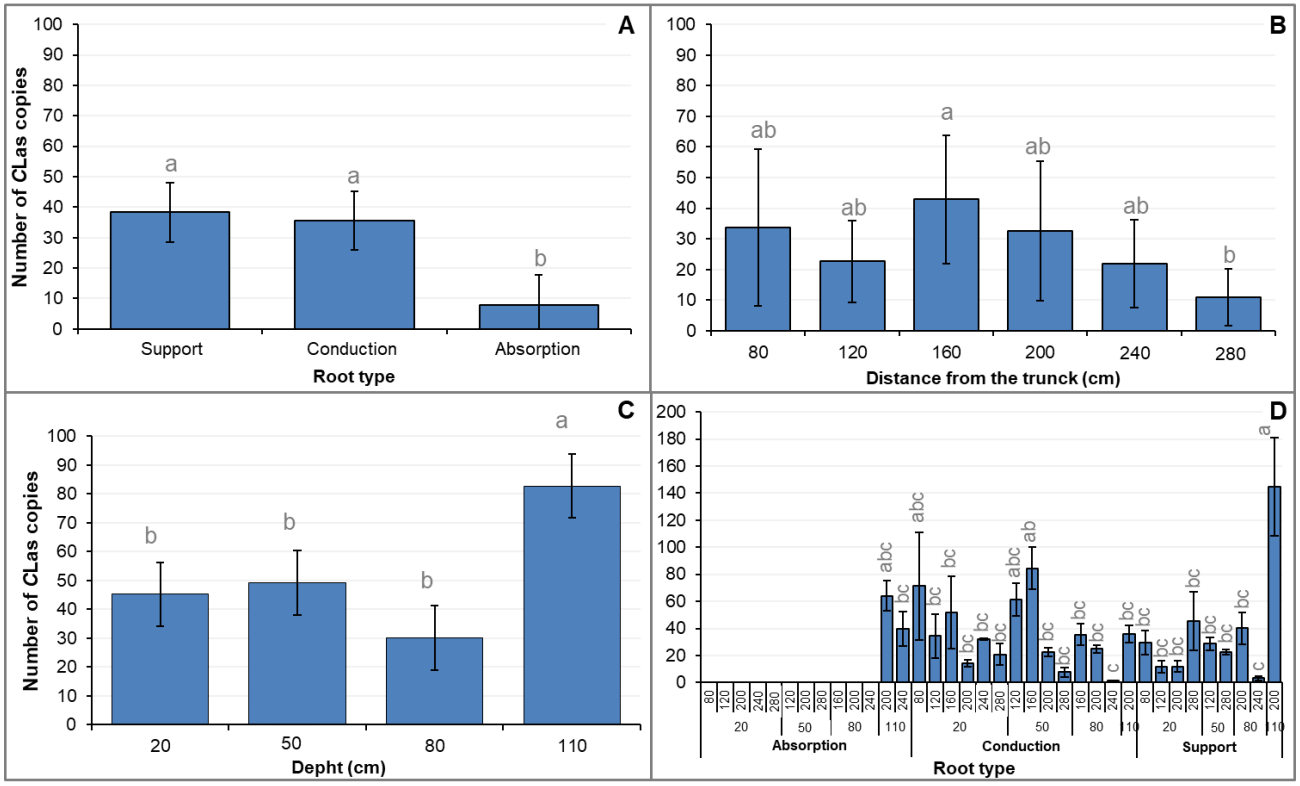

Figure 6. A. Quantification of *C*Las by root type: *support, conduction*, and *absorption* in HLB-asymptomatic *C. sinensis* / *C. aurantium* A3-tree. **B.** Quantification of *C*Las in six sectional distances from the trunk between 80 and 240 cm. **C.** Quantification of *C*Las in four sectional soil depth between 20–110 cm. **D.** Quantification of *C*Las integrating the three factors of root type, distance, and depth. Standard deviation bars with different letters were statistically different using ANOVA and *Tukey's* mean comparison ($p = 0.05$).

Spatial geostatistical simulation of *C*Las. The *C*Las concentration in the root system showed various distribution and mobility scenarios (Figure 3 and 7). In general, two sections of greater intensity and inoculum load concentration (80 – 144 copies) were observed, associated with the middle canopy-drip zone (140 – 220 cm) and medium depth strata (40 – 80 cm) (Figure 7A). The geostatistical interpolation model showed the highest intensity gradient (144 copies) between sections of *conducting* roots in the middle drip zone of the canopy. A second high-intensity gradient (>80 *C*Las copies) was in the absorption root section (Figure 7A). A second high-intensity gradient (>80 *C*Las copies) was in the *absorption root* section (Figure 7A).

The simulation of *C*Las mobility using the *Grid Vector Map* geostatistical analysis showed that the two sections of bacterial concentration were associated with mobility patterns differentiated by the type of colonized root. The first, between 140 – 160 cm from the main axis and 20 – 65 cm deep, was associated with incidence in *conducting* roots (d = 6.38 mm). In this section, the mobility pattern with the highest inoculum load (size and red color of the vector) was toward a trunk distance of 160 – 200 cm and a soil depth of 40 – 60 cm. The second was between 180 – 240 cm and 80 – 110 cm, respectively, associated with *support* roots (d = 18 mm) and *absorption* roots (d = 1.5 mm) with an upward mobility pattern from soil depth strata at 110 cm to 20 – 40 cm (Figure 7B).

The incidence in *supporting* roots showed a decreasing gradient of *C*Las (30 – 118 copies) at depths greater than 40 cm towards the 220 cm zone relative to the trunk of *C. sinensis*. The highest *C*Las load and intensity (90 – 114 copies) was associated with 70 – 110 cm depth and at 200 – 250 cm distance from the trunk (Figure 7C). The *C*Las load in *conducting* roots showed variable and random mobility patterns on the three-dimensional soil core analyzed, suggesting greater mobility and less restrictiveness due to the abundance and wide distribution in the root structure.

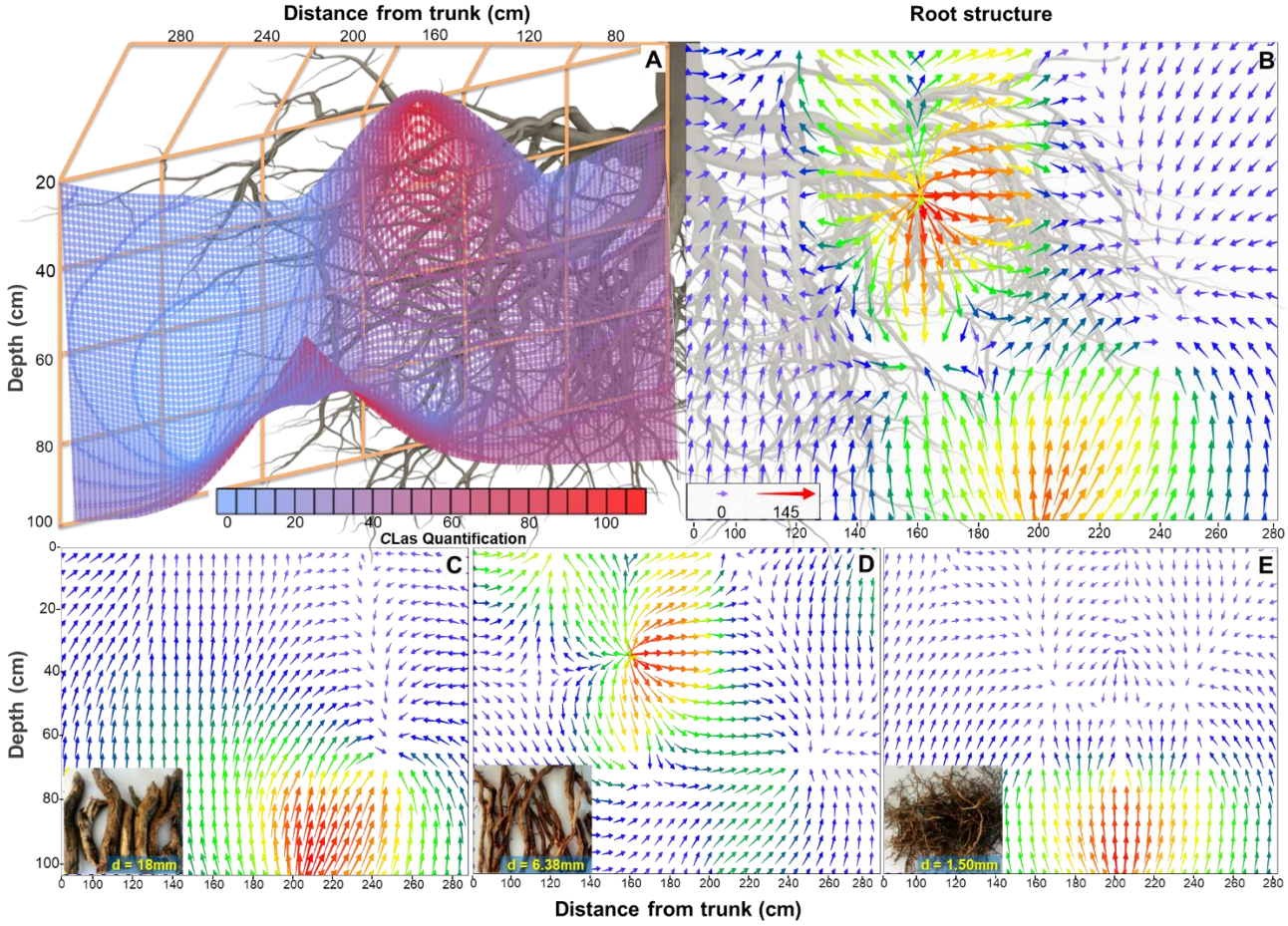

Figure 7. A. *3D wireframe* geostatistical interpolative analysis of the quantification of *C*Las associated to a 3D sectional sampling system in *support* (d = 18 mm), *conduction* (d = 6.3 mm), and *absorption* roots (d = 1.5 mm) in Valencia *C. sinensis* / *C. aurantium* A3-tree. **B-E**. *Grid Vector Map* geostatistical analysis to represent the concentration and mobility of *C*Las bacterium load in total root samples (**B**), *support* (**C**), *conduction* (**D**), and *absorption* (**E**). The vector size and color show the inoculum load by root type and spatial sector. The directionality and magnitude (size) of vectors show the simulation of *C*Las mobility and concentration on the root structure. On bottom box (**B**), the numbers of bacterium copies relate to the arrows size and color as reference measure.

The bacterium load gradient (30 – 71 copies) for *conducting* roots was mainly associated with 20 – 60 cm depth and 80 – 160 cm distance of the trunk, with a lower intensity and inoculum load (20 – 25 copies) between 80 – 100 and 200 – 240 cm distance (Figure 7D). In *absorption* roots, the highest inoculum load and mobility capacity was associated with soil depth strata between 80 – 110 and 80 – 280 cm from the trunk, although *absorption* roots are likely to be predominant on the surface and at the periphery of the root system. The highest inoculum load (31–70 copies) was concentrated at 160 – 240 cm distance. The mobility pattern was upward, with a predominance from 110 cm to the 60 cm depth stratum. With a lower bacterial load (5 – 18 copies), a peripheral dispersion pattern was evident, converging at medium depth and distance from the trunk (Figure 7E).

DISCUSSION

The hypothesis of asymptomatic HLB associated with a prolonged *incubation period* (*IP*) in response to infection by *Candidatus* Liberibacter asiaticus (*C*Las) on 30-years-old Valencia orange trees (*C. sinensis* / *C. aurantium*), from a commercial orchard in the Central Gulf of Mexico, was analyzed by measuring the concentration and spatiotemporal distribution of the bacteria in the canopy and three root types under confinement conditions. During seven monthly evaluations, a total of 1540 samples were analyzed. No visual symptoms were observed despite detection of 39.4 – 49.5% qPCR-positive samples well distributed in canopy, and in proximal (50.9%) and distal (49.1%) branches. The lack of symptoms for at least 7 months contrasts with the incubation of *C*Las for two to five months in 1.5-year-old *C. sinensis* / *C. limonia* plants after infection with infectious *Diaphorina citri* (Canale *et al*., 2020). However, the incubation associated with a presymptomatic condition of HLB is variable in citrus and has been reported to range from months to years, depending on vector population density, inoculum load, plant age, graft / rootstock, detection in commercial orchards or backyards, among other epidemiological factors (Gottwald *et al*., 2010). However, several of these reports have been empirical estimates or without experimental support.

In this study, the *incubation period* refers to the time between successful infection via *D. citri* and the expression of the first visible HLB symptoms. In this case, due to the novel experiment developed for a natural asymptomatic condition in the field, the infection could not be controlled and therefore time-*0* was unknown. However, the premise was that the bacteria concentration should be incremental and gradually exhibit a chronic systemic canopy-root colonization if the asymptomatic condition was transient and explained by a prolonged *incubation period*. The objective was not to estimate the *incubation period*, but to analyze this event as the cause of the symptom's expression delay.

Initial characteristic visible symptoms on foliage, following infection by *C*Las, also contrast depending on the citrus species, climatic conditions, inoculum source load, and other factors (Canale *et al*., 2020; Esquivel-Chávez *et al*., 2012; Lopes *et al*., 2009). In chronic asymptomatic HLB, symptoms are not a reference parameter for determining *IP*, especially when high bacterial concentrations (1 x 10^9 copies) and low thresholds for *C*Las acquisition by *D. citri* (2694 copies) have been demonstrated under natural spreading in commercial orchards (G. Mora, unpublished). Complementarily, *IP* is part of the pathogenesis process *sensu* Vanderplank, conceived for local infections with visible symptoms / signs (*e.g.*, fungy), not for systemic infections such as those caused by *C*Las. Consequently, the latency period (*LP*) in *C*Las, classically understood as the time required for a pathogen to produce new inoculum from the first visible symptom, has been indirectly inferred from the *D. citri* ability to acquire *C*Las and infect new plants, resulting in periods

up to 1 month shorter than *IP* (Canale *et al*., 2020). This implies that *LP* is not successive and synchronous with *IP sensu* Vanderplank and that understanding pathogenesis in a systemic infection requires another histological-mechanistic framework (Esquivel-Chávez, 2016; Esquivel-Chávez *et al*., 2012). In this research, *IP* was inferred through inoculum dynamics, *i.e.,* multiplication and distribution in the host.

Although these methodological and biological restrictions highlight the complexity of explaining asymptomatic HLB using *PI*, a critical aspect is to determine whether the space-time dynamics of bacterial concentration can determine a chronic, *i.e.*, permanent, asymptomatic condition or a transient condition leading to the eventual expression of visible symptoms. For example, the intensity in HLB symptomatic expression, and consequently in concentration, has been associated with environmental variables (temperature and RH) and bacterial migration to the root (Bassanezi *et al*. 2013b).

The concentration of *C*Las in warm regions of São Paulo, Brazil, was related to high temperature and RH (Lopes *et al*., 2009). In S.J. Acateno, the highest incidence of samples (37 – 87 positive) and *C*Las concentration (2.1 – 3.5 log) was associated with significant temperature variation of 19.1 – 27.6 °C ($\overline{x}$ = 24.4 ± 3.0) and moderate to high humidity 74.4–98.7 RH ($\overline{x}$ = 89.2 ± 10.2). In contrast, the *C*Las decremental phase was mainly associated with lower temperature range of 12.1 – 23.6 °C ($\overline{x}$ = 19.1 ± 2.6) than with humidity (79.7 – 98.9 RH, $\overline{x}$ = 92.0 ± 7.5).

In general, at canopy level, a temporal effect of *C*Las was observed ($p < 0.0001$), with summer samples having a significantly higher concentration (2.1 – 3.5 log-*C*Las) compared to spring and fall-winter (≤ 1.8 log-*C*Las). Note, however, that temperatures in S.J. Acateno are not extreme and the summer effect may be reversed at other latitudes. Other studies have reported differences between seasons, validating the seasonal bacterium fluctuation in symptomatic commercial orchards (Sauer *et al*., 2015). These results indicate that temperature is involved in *C*Las concentration variation but does not explain an asymptomatic effect by *IP*.

The premise of attributing asymptomatic status to prolonged *IP*, inferred by incremental inoculum load over time and canopy-root space, was also ruled out in this investigation. The concentration of *C*Las fluctuated in the range of 1.5 – 3.5 log copies / reaction 100 mL during the evaluation period (range = 6.3 – 68870.7 copies). *C*Las studies using controlled infection in young *C. sinensis* Pera plants suggest stability in visual detectability at approximately 5 log cells g^{-1} 40 days after inoculation and a minimum threshold of 2.6 log (2.6 – 3.6 log *C*Las) for symptom expression in new shoots, 24 days after inoculation (Cui *et al*., 2022; Alves *et al.*, 2021). Although in this study the results exceeded that threshold for at least two continuous monthly periods and up to four discontinuous periods, the asymptomatic condition was maintained.

At the branch-sector or canopy-sector level, the concentration of *C*Las was statistically different (p = 0.07). Branches showed heterogeneous inoculum loads between sectors, reaching up to 2.4 – 5.1 log-*C*Las. This effect has been observed in Brazil in commercial fields on adult trees of different *C. sinensis* cultivars with contrasting variations in Ct's in canopy quadrants (Sauer *et al*., 2015), evidencing high intra-plant variability and the need for additional studies on the processes of infection and colonization of *C*Las in plants (Raiol-Junior *et al*., 2020), especially in commercial orchard conditions.

The epidemic inoculum load parameterization ($\boldsymbol{Y_i}$, $\boldsymbol{Y_{max}}$, and $\boldsymbol{Y_f}$) of *C*Las concentration curves validated the temporal fluctuation of the bacteria, which was neither incremental nor gradual over the canopy, reinforcing the null or low effect of *IP* in the HLB-

asymptomatic condition. The highest positivity and concentration of *C*Las ($\mathbf{Y_{max}}$) was found to be associated with the upper-middle sector of the canopy. The inoculum in the initial phase ($\boldsymbol{Y_i}$) and final epidemic phase ($\boldsymbol{Y_f}$) showed mobility towards the lower and lower-upper sectors, respectively. The effect of higher concentration in the middle-upper sector may be associated with the emission of shoots and tissue renewal (Raiol-Junior *et al*., 2020), which can be asymptomatic reservoirs of the bacteria and a source of acquisition and dispersal by the insect vector. Lee and coworkers (2015) simulated that in approximately one year, up to 12 000 individuals of *D. citri* / tree can be infectious (Lee *et al*., 2015).

At the genetic recognition level, the temporal and spatial expression of *C*Las effectors (*e.g.*, CLIBASIA_03875, CLIBASIA_04800, CLIBASIA_05640, etc.) should also be considered in early colonization, suppression of tolerance genes, and long-term survival, potentially involved in an asymptomatic or presymptomatic condition (Shi *et al*., 2019).

The asymptomatic condition associated with the movement of *C*Las towards the root is a biologically and epidemiologically relevant factor (Bassanezi *et al*. 2013b). Recent studies have documented the movement of *C*Las towards newly developed root and leaf tissues (Raiol-Junior *et al*., 2020). However, the root factor has been little studied directly in the field due to the prioritization of visual symptom diagnosis, PCR genomic methods, and the difficulty of root sampling due to its complex structure in *Citrus* spp. (Alves *et al*., 2021).

The detection of *C*Las in young plants roots can precede an undetectable and asymptomatic condition in foliage, and it can be up to three times more efficient than in leaves (Xie *et al*., 2021; Braswell *et al*., 2020; Raiol-Junior *et al*., 2020; Graham *et al*., 2014; Johnson *et al*., 2013). This was not the case in these results, supporting the idea that *PI* is not mechanistically involved. Overall, *C*Las had a widespread distribution in canopy and roots. The probability of detecting *C*Las in roots vs. tissue was not statistically different (38.7 vs. 41.9%, $p < 0.05$), but there were differences in inoculum load ($p = 0.0001$) with 9 – 43.4 vs. 6.3 – 68 870.7 copies in asymptomatic leaf tissue. There was also an effect of root type with 47.6, 15.4, and 38.7% of positive samples out of a total of 111, and 38.3, 43.4, and 9.5 average copies of *C*Las for *support*, *conduction*, and *absorption* roots, respectively ($p < 0.0001$). In contrast, Raiol-Junior *et al*. (2020), who worked under controlled environment conditions with Pera 60-cm-plants *C. sinensis* / *C. volkameriana*, found that young roots (*absorption*) had the highest bacterial load after root pruning.

It is important to point out that results of *C*Las dynamics are inherent to the initial inoculum-plant interaction without the influence of external inoculum sources, since reinfection events with *D. citri*, and eventual transmission of other *C*Las variants associated with greater aggressiveness (G. Mora, unpublished), were excluded by tree confining.

Other factors, such as the vector density effect, *C*Las variant, and graft / rootstock combination could not be ignored in studies of an asymptomatic condition. For example, in S.J. Acateno, Puebla, low populations of *D. citri* were recorded, with an average of 2.9 – 3.2 insects per yellow sticky trap during periods with the highest detection of positive canopy samples, significantly lower than in high-density populations in regions such as Tecomán, Colima, with 18.3–56.1, and Martínez de la Torre, Veracruz, with 5.4–7.9 *D. citri* per trap on average (SIMDIA, 2022). Similarly, under chronic - endemic conditions since 2010 in Mexico (Mora-Aguilera *et al*., 2014), the bacterial load has been notably high, exceeding 2.5×10^7 *C*Las copies in *C. aurantifolia* / *Macrophylla* or *Volkameriana*

in Colima or Michoacán (De la Rosa, 2016), compared to a range of 6.3 - 68 870.7 copies in this study.

Another consideration in the presymptomatic condition is the structural modification of the phloem in infected tissue, *e.g.*, starch accumulation, cell wall thickening, expression of callose genes and proteins (*e.g.*, CALLOSE SYNTHASE7 and PHLOEM PROTEIN2), resulting in differential plugging of vascular bundles depending on the type of *Citrus* spp. / rootstock rather than inoculum load or *C*Las intra-plant movement (Cavichioli *et al*., 2022; Xie *et al*., 2021; Achor *et al*., 2020). This behavior was reported in palisade and spongy parenchyma of *C. aurantifolia* symptomatic tissue compared to that of *C. sinensis*. In particular, the phloem area and width in asymptomatic tissue of infected plants was 1.9 times smaller in sweet orange (Esquivel-Chávez *et al*., 2012).

These results provide evidence that *PI* does not explain the asymptomatic condition of *C*Las in the productive environment of S.J. Acateno. Additionally, it reinforces the importance of designing strategies to establish efficient surveillance-monitoring systems for the detection of *C*Las in chronic or transient asymptomatic conditions. Likewise, they generate new management perspectives based on the genetic understanding of plant-pathogen interaction and epidemic implications. This is the first study to mechanistically analyze *IP* at the canopy - root level, in initial detections of asymptomatic HLB in Mexico in adult productive trees of Valencia *C. sinensis* / *C. aurantium* under field condition.

CONCLUSIONS

This work is part of a broad investigation conducted by the CP-LANREF group, focused on analyzing for the first time the asymptomatic condition of HLB in sweet orange / N. agrio. Specifically, this work demonstrated that a prolonged *incubation period* does not determine the asymptomatic condition based on the spatiotemporal variation of *Candidatus* Liberibacter asiaticus concentration at the canopy-root plant level.

The asymptomatic positive condition of *C*las was maintained through seven monthly evaluations of aerial tissue and a comprehensive root evaluation. The concentration was fluctuating, not incremental, with statistical differences according to seasonality or root type. The relatively homogeneous distribution of *C*Las in the tree canopy and the presence of this bacterium in *support*, *conduction*, and *absorption* roots suggests a chronic medium- to long-term infection, so the absence of visible symptoms may have other physiological, histological, or genetic causes inherent to the pathogen. Additionally, the eventual occurrence of symptoms in asymptomatic trees should consider reinfection by variants and changes in the population structure of the pathogen. These results contribute to strengthening surveillance-monitoring strategies by seasonality, canopy-branch sectors, and tissue type with a higher probability of detection even in asymptomatic conditions and generate new insights for *C*las management.

Limitations

This work was carried out over seven months on commercial sweet orange/bitter orange trees over 30 years old in the Central Gulf region of Mexico. The effect of other production and climatic conditions on a possible asymptomatic condition of HLB is unknown.

Conflict of interest. Research was conducted with not involved conflicts.

Funding. To SECIHTI (formerly CONACYT) for the scholarship to graduate students and to SENASICA-DGSV for the funding to carry out this research. To COLPOS for the financial and logistic facilities.

Acknowledgments

To the State Plant Health Committee of Puebla for logistical and technical support. To the citrus producers of San José Acateno, Puebla for facilitating the research. To Miguel Trujano Guzman for field work on sampling and plant caging. To the CP-LANREF team for their enthusiastic technical and scientific involvement.

Contribution of the authors

GMA, conception, analysis and interpretation of results, final drafting; GAS, statistical analysis and drafting; VMB and VLB, sampling and PCR analysis; MAGE, interpretation of results and document review; PRG, conception and financial and operational management.

REFERENCES

Achor D, Welker S, Ben-Mahmoud S, Wang C, Folimonova SY, *et al.* 2020. Dynamics of *Candidatus* Liberibacter asiaticus movement and sieve-pore plugging in Citrus sink cells. Plant Physiology 182(2):882–891. https://doi.org/10.1104/pp.19.01391

Alves MN, Cifuentes-Arenas JC, Raiol-Junior LL, Ferro JA and Peña L. 2021. Early population dynamics of "*Candidatus* Liberibacter asiaticus" in susceptible and resistant genotypes after inoculation with infected *Diaphorina citri* feeding on young shoots. Frontiers in Microbiology 12: 683923. https://doi.org/10.3389/fmicb.2021.683923

Bassanezi RB, Montesino LH, Gimenes-Fernandes N, Yamamoto PT, Gottwald TR, *et al*. 2013a. Efficacy of area-wide inoculum reduction and vector control on temporal progress of huanglongbing in young sweet orange plantings. Plant Disease 97: 789-796. https://doi.org/10.1094/PDIS-03-12-0314-RE

Bassanezi RB, Belaque JJ and Montesino LH. 2013b. Frequency of symptomatic trees removal in small citrus blocks on citrus huanglongbing epidemics. Crop protection 52: 72-77. https://doi.org/10.1016/j.cropro.2013.05.012

Bassanezi RB, Busato LA, Bergamin Filho A, Amorim L and Gottwald TR. 2005. Preliminary spatial pattern analysis of huanglongbing in São Paulo, Brazil. Pp: 341–55 *In:* Proceedings of the 16th Conference of the International Organization of Citrus Virologists. Riverside, CA, USA: IOCV. https://iocv.ucr.edu/publications/proceedings#proceedings-16-2005-conference

Braswell WE, Park JW, Stansly PA, Kostyk BC, Louzada ES, *et al*. 2020. Root samples provide early and improved detection of *Candidatus* Liberibacter asiaticus in Citrus. Scientific Reports 10:16982. https://doi.org/10.1038/s41598-020-74093-x

Canale MC, Komada KMA and Lopes JRS. 2020. Latency and incubation of '*Candidatus* Liberibacter asiaticus' in citrus after vector inoculation. Tropical Plant Pathology 45: 320–326. https://doi.org/10.1007/s40858-019-00311-1

Cavichioli TM, Curtolo M, Cristofani-Yaly M, Rodrigues J and Coletta-Filho HD. 2022. Temporal analysis of *Candidatus* Liberibacter asiaticus in *Citrandarin* genotypes indicates unstable Infection. Agronomy 12(10):2566. https://doi.org/10.3390/agronomy12102566

Cui X, Zhang J, Liu Y, Luo X, Deng X, *et al*. 2022. Comparison of different grafting methods on the effect of '*Candidatus* Liberibacter asiaticus' transmission. Fruit Research 2:15 https://doi.org/10.48130/FruRes-2022-0015

De la Rosa AA. 2016. Distribución de la Carga de Inóculo Regional de *Candidatus* Liberibacter asiaticus en *Diaphorina citri* en Tres Escenarios Citrícolas de México. Colegio de Postgraduados Montecillo. Tesis MC. 101 p. http://colposdigital.colpos.mx:8080/xmlui/handle/10521/4144

Esquivel-Chávez F. 2016. Dinámica de la Concentración Bacteriana de *Candidatus* Liberibacter asiaticus y su Efecto en la Expresión Sintomática e Histológica en Cítricos Agrios y Dulces e Implicaciones en el Potencial de Inóculo. Colegio de Postgraduados. Tesis DOC. 165 p.

Esquivel-Chávez F, Valdovinos-Ponce G, Mora-Aguilera G, Gómez-Jaimes R, Velázquez-Monreal JJ, *et al*. 2012. Análisis histológico foliar de cítricos agrios y naranja dulce con síntomas ocasionados por *Candidatus* Liberibacter asiaticus. Agrociencia 46(8): 769-78. http://www.redalyc.org/articulo.oa?id=30225072002

Esquivel-Chávez F. 2011. Análisis Histológico y Epidemiológico de Limón Mexicano y Limón Persa Asociados a Síntomas del HLB (Huanglongbing). Tesis de Maestría. Colegio de Postgraduados, Texcoco Edo. de México. 56 p.

Flores-Sánchez JL, Mora-Aguilera G, Loeza-Kuk E, López-Arroyo JI, Gutiérrez-Espinosa MA, *et al*. 2017. Diffusion model for describing the regional spread of Huanglongbing from first-reported outbreaks and basing an area wide disease management strategy. Plant Disease 101:1129-1127. https://doi.org/10.1094/PDIS-04-16-0418-RE

Flores-Sánchez JL, Mora-Aguilera G, Loeza-Kuk E, López-Arroyo JI, Domínguez-Monge S, *et al*. 2015. Yield loss caused by *Candidatus* Liberibacter asiaticus in Persian lime, in Yucatan Mexico. Mexican Journal of Phytopathology 33: 195-210. https://www.redalyc.org/articulo.oa?id=61242145005

Gottwald T, Luo W, Riley T and Parnell S. 2014. Edge effect and Huanglongbing. Journal of Citrus Pathology 1: 126-127. https://doi.org/10.5070/C411024824

Gottwald TR. 2010. Current epidemiological understanding of Citrus Huanglongbing. Annual Review of Phytopathology 48: 119-139. https://doi.org/10.1146/annurev-phyto-073009-114418

Graham JH, Johnson EG, Gottwald TR and Irey MS. 2014. *Candidatus* Liberibacter asiaticus causes damage to citrus fibrous roots before visual decline of Huanglongbing-infected citrus trees. Journal of Citrus Pathology 1(1). http://dx.doi.org/10.5070/C411025122

Johnson EG, Wu J, Bright DB and Graham JH. 2013. Association of '*Candidatus* Liberibacter asiaticus' root infection, but not phloem plugging with root loss on huanglongbing-affected trees prior to appearance of foliar symptoms. Plant Pathology 63(2): 290-298. https://doi.org/10.1111/ppa.12109

Lee JA, Halbert SE, Dawson WO, Robertson CJ, Keesling JE, *et al*. 2015. Asymptomatic spread of Huanglongbing and implications for disease control. Plant Health 112(24): 7605-7610. https://doi.org/10.1073/pnas.1508253112

Li W, Hartung JS and Levy L. 2006. Quantitative real-time PCR for detection and identification of *Candidatus* Liberibacter species associated with Citrus Huanglongbing. Journal of Microbiological Methods 66:104-115. https://doi.org/10.1016/j.mimet.2005.10.018

Lopes SA, Bertolini E, Frare GF, Martins EC, Wulff NA, *et al*. 2009. Graft transmission efficiencies and multiplication of '*Candidatus* Liberibacter americanus' and '*Ca*. Liberibacter asiaticus' in citrus plants. Phytopathology 99:301–306. https://doi.org/10.1094/PDIS-11-12-1031-RE

Mora-Aguilera G, Robles-García P, López-Arroyo JI, Velázquez-Monreal JJ, Flores-Sánchez JL, *et al*. 2014. Current situation and prospects for management of citrus HLB. Mexican Journal of Phytopathology 32(2): 108-119. http://www.redalyc.org/articulo.oa?id=61243856003

Raiol-Junior LL, Cifuentes-Arenas JC, de Carvalho EV, Girardi EA and Lopes SA. 2020. Evidence that '*Candidatus* Liberibacter asiaticus' moves predominantly toward new tissue growth in Citrus plants. Plant Disease 105:34-42. https://doi.org/10.1094/PDIS-01-20-0158-RE

Robles-González MM, Velázquez-Monreal JJ, Manzanilla-Ramírez MA, Orozco-Sánchez M, Medina-Urrutia VM, *et al*. 2013. Síntomas del huanglongbing (HLB) en limón mexicano (*Citrus aurantifolia*) y su dispersión en el estado de Colima, México. Revista Chapingo Serie Horticultura 19(1): 15-31. http://www.redalyc.org/articulo.oa?id=60926253002.

Sauer AV, Zanutto CA, Requena NPT, Machado MA, Bock CH, *et al*. 2015. Seasonal variation in populations of '*Candidatus* Liberibacter asiaticus' in citrus trees in Paraná State, Brazil. Plant Disease 99(8): 1125-1132. https://doi.org/10.1094/PDIS-09-14-0926-RE

SENASICA. 2022. Primer Informe Semestral 2022 Campaña de Protección Fitosanitaria para Plagas de los Cítricos. 10 p. https://www.gob.mx/cms/uploads/attachment/file/757852/1er__Informe_semestral_2022_Plagas_de_C_tricos.pdf

SENASICA. 2015. Acciones contra el Huanglongbing y su vector en México. Informe Julio, 2015. http://www.senasica.gob.mx/?doc=26771

SENASICA. 2012. Cambio de estatus fitosanitario de HLB en Veracruz. https://www.gob.mx/senasica/prensa/cambio-de-estatus-fitosanitario-de-hlb-en-veracruz

SENASICA. 2010. Protocolo de actuación ante la emergencia por la detección del Huanglongbing. 2ª Edición. Dirección General de Sanidad Vegetal, México. http://www.senasica.gob.mx/?doc=9364.

Shi Q, Pitino M, Zhang S, Krystel J, Cano LM, *et al*. 2019. Temporal and spatial detection of *Candidatus* Liberibacter asiaticus putative effector transcripts during interaction with Huanglongbing-susceptible, -tolerant, and -resistant citrus hosts. BMC Plant Biology 19:122. https://doi.org/10.1186/s12870-019-1703-4

SIMDIA. 2022. Sistema de Monitoreo de *Diaphorina*. DGSV-SENASICA. http://www.siafeson.com/simdia/

Xie Z, Zhao K, Long J, Zhen L, Zou X, *et al*. 2021. Comparative analysis of Wanjincheng orange leaf and root responses to '*Candidatus* liberibacter asiaticus' infection using leaf-disc grafting. Horticultural Plant Journal 7(5): 401-410. https://doi.org/10.1016/j.hpj.2021.01.007